

1 Design and simulation of an integrated process for biodiesel production from  
2 waste cooking oil using supercritical methanolysis

3 *Omar Aboelazayem<sup>a,b</sup>, Mamdouh Gadalla<sup>c,a,1</sup> and Basudeb Saha<sup>b</sup>*

4 <sup>a</sup> Department of Chemical Engineering, The British University in Egypt, Misr-Ismalia Road, El-  
5 Shorouk City 11837, Cairo, Egypt.

6 <sup>b</sup> Centre for Energy and Environment Research, School of Engineering, London South Bank  
7 University, 103 Borough Road, London, SE1 0AA, UK.

8 <sup>c</sup> Department of Chemical Engineering, Port Said University, Port Said, Egypt.

9  
10 **ABSTRACT**

11 Non-catalytic transesterification has been recognised as an effective technique for biodiesel  
12 production. It has many advantages over conventional catalytic transesterification, where it  
13 eliminates the difficulties of catalysts preparation and separation. It also produces high  
14 biodiesel yield in shorter reaction time. However, it requires harsh operating conditions at  
15 high reaction temperature and pressure, in addition to using large excess of methanol. In an  
16 attempt to mitigate these problems, a process design/integration for biodiesel production has  
17 been performed. The process has been subjected to both mass and energy integration to  
18 minimise fresh methanol requirements and to minimise heating and cooling energies,  
19 respectively. A new graphical Pinch Analysis method has been used to evaluate the energy  
20 performance of a literature design for the current process. It has been subsequently used to  
21 develop an optimum heat exchanger network (HEN) for the process by matching of process  
22 streams. Also, the design made by using an automated commercial simulation (Aspen Energy  
23 Analyzer) has been evaluated using the same graphical method. The produced HEN design  
24 from graphical method has achieved the optimum results with respect to energy targets.

25  
26 **KEYWORDS**

27 Biodiesel, Waste cooking oil, Graphical Pinch Analysis, Heat integration, Mass integration.

28  
29 **HIGHLIGHTS**

- 30
- 31 • Design and simulation of an integrated process for biodiesel production.
  - 32 • Heat and mass integration have been applied to improve process performance.
  - 33 • An optimum HEN has been developed using graphical Pinch method.
  - Previous HEN designs have been evaluated using new graphical Pinch method.

**Corresponding Author**

<sup>1</sup> (M. Gadalla). Email: mamdouh.gadalla@bue.edu.eg

## 34 1. INTRODUCTION

35 Diesel fuel is the most consumed fuel over other petroleum products where it is used  
36 extensively in transportation sector and energy generation [1]. Consequently, biofuels with  
37 similar properties to diesel fuel are considered the future of energy resources as they could  
38 be implemented directly to the existing diesel engines with minor or without modifications  
39 [2]. Biodiesel has been considered as the most promising substitute for petroleum diesel fuel.  
40 It is a biomass-derived fuel from vegetable oils, animal fats and recently from micro-algae.  
41 Biodiesel is defined as mono alkyl esters of long chain fatty acids derived by alcoholysis of  
42 triglycerides from different feedstocks [3]. Biodiesel is characterised by its biodegradability,  
43 low emissions of particulates, carbon monoxide and hydrocarbons, absence of sulphur  
44 emission and high cetane number [4]. The similar properties of biodiesel to petroleum diesel  
45 besides being a sustainable green fuel have promoted biodiesel as a significant alternative  
46 fuel for petroleum diesel.

47 Transesterification reaction has been considered the most commonly used method for  
48 biodiesel synthesis. The reaction is usually catalysed using different techniques including  
49 alkaline, acidic and biological catalysts [5]. Recently, non-catalytic transesterification has  
50 been reported using supercritical alcohols [6]. Origin and quality of the feedstock are  
51 responsible for selecting the processing technique. Presently, edible oils are considered the  
52 main feedstock for biodiesel. However, the raising competition with food industry resulted  
53 in food insecurity has boosted the research towards non-edible and waste oils (second  
54 generation feedstock). The second generation feedstock is considerably cheaper than edible  
55 oil, which contributes in lowering the overall cost of the produced biodiesel [7].

### List of Abbreviations:

WCO, waste cooking oil; FFA, free fatty acid; NaOH, sodium hydroxide; KOH, potassium hydroxide; DMC, dimethyl carbonate; MTBE, methyl *tert*-butyl ether; CSTR, continuous stirred tank reactor; FAME, fatty acid methyl ester; CO<sub>2</sub>, carbon dioxide; TAN, total acid number; TG, triglycerides; NRTL, non-random two liquids; EOS, equation of state; k, reaction rate constant; HEN, heat exchanger network; MEN, mass exchanger network; VDU, vacuum distillation column.

56 Waste cooking oil (WCO) has been recognised as a potential feedstock for biodiesel as it is  
57 relatively cheaper than fresh edible oils and it contributes in waste utilisation [8]. However,  
58 the high free fatty acids (FFA) and water content are the main drawbacks of using WCO as  
59 a feedstock. Alkaline homogenous catalysed technique, using either sodium hydroxide  
60 (NaOH) or potassium hydroxide (KOH), is considered the most commonly used technique  
61 for biodiesel synthesis. The high FFA content in WCO leads to saponification reaction while  
62 using alkaline homogenous catalysts, which results in lowering biodiesel yield and  
63 preventing product separation. Using heterogeneous catalyst prevents saponification side  
64 reaction. However, it is very sensitive even at low water content in addition to high cost of  
65 catalyst preparation as it requires extremely harsh conditions (700-900°C). Two-steps  
66 transesterification is considered as an acceptable technique for producing biodiesel from  
67 WCO. A pre-treatment esterification of FFA step using acidic catalysts is followed by  
68 transesterification step using alkaline homogenous catalysts. Nevertheless, the lengthy  
69 process leads to increase in biodiesel cost [9].

70 Non-catalytic transesterification has been considered as an ideal technique for biodiesel  
71 production from WCO as it prevents all the above-mentioned problems. It tolerates both  
72 esterification of FFA and transesterification of triglycerides in a single step reaction.  
73 However, it requires high reaction temperature and pressure, where the alcohol should be at  
74 the supercritical state [10]. Several supercritical technologies have been used for non-  
75 catalytic production of biodiesel using methanol, ethanol, 1-propanol, dimethyl carbonate  
76 (DMC), methyl *tert*-butyl ether (MTBE) and methyl acetate [11,12].

77 West et al [13] have designed and simulated four biodiesel production processes using  
78 different techniques including homogenous alkaline catalysed, homogenous acidic catalysed,  
79 heterogeneous alkaline catalysed and non-catalytic supercritical processes. They have also  
80 performed an economic comparative analysis between the designed processes for the cost of  
81 production 8000 tonne/y of biodiesel from WCO. They have concluded supercritical process  
82 as the second most profitable process next to heterogeneous catalysed process. Lee et al [10]  
83 have simulated production process for biodiesel using both fresh and used cooking oils. They  
84 have reported that the cost of the feedstock attributes with about 64-84% of the produced  
85 biodiesel cost. They have also reported that using supercritical methanol is the most  
86 economically favourable process over alkaline catalysed processes. Manuale et al [14] have  
87 simulated an energy-integrated biodiesel production process using supercritical methanol.  
88 They have proposed that using the enthalpy content of the reactor product stream to separate

89 most of the unreacted methanol in a flash drum decreased the process required heating  
90 energy.

91 Pinch technology is recognised as one of the most effective methods used to assess the  
92 efficiency of energy utilisation for production processes. The idea was proposed in 1978 by  
93 Umeda et al [15] which has been developed for further aspects by Linnhoff and Hindmarch  
94 [16]. The principle has been subsequently extended into several areas including mass Pinch,  
95 hydrogen Pinch and water Pinch. Smith [17] has discussed the principles for Pinch Analysis  
96 which have been implemented in mass and energy integration applications and extensively  
97 applied in heat recovery. The applications of such principles are very critical for providing  
98 energy and mass targets that should ideally be achieved in a process [18]. El-Halwagi [19]  
99 has introduced systematic and graphical procedures based on Pinch Analysis to design both  
100 mass and heat exchanger networks in complicated process industries.

101 Process integration for energy or materials savings can be achieved through two approaches,  
102 one which is based on insights derived from Pinch Analysis and the other is based on  
103 mathematical programming methodologies. The first approach normally comprises of two  
104 stages, first determining the energy (or mass) targets known as targeting, and then designing  
105 the heat and/or mass exchanger network to achieve these targets [20]. The mathematical  
106 programming-based approach relies on building superstructure for all alternatives and then  
107 using simultaneous optimisation and integration to explore all interconnection within the  
108 proposed superstructure. This is followed by screening of all the alternative to find the  
109 optimal combination [21,22]. The recent handbook of Klemes [23] is a good source for such  
110 literature.

111 Gadalla [24] has reported a novel graphical technique for HEN designs based on Pinch  
112 technology. The graphical method has been defined by plotting process hot streams *versus*  
113 process cold streams. Each process heat exchanger has been represented by a straight line  
114 where its slope the is function of the ratio between heat flows and capacities. In addition,  
115 each line is proportional to the flow of the heat transferred across the exchanger. This method  
116 could easily analyse any proposed HEN to identify inappropriate exchangers whether across  
117 the Pinch, network Pinch and improper placements. In addition, he reported that the  
118 developed method could be implemented in designing optimum HENs using numerical  
119 process streams matching technique. Gadalla [25] has also extended the same conceptual  
120 novel graphical method for mass integration applications and mass exchanger networks  
121 (MEN) designs.

122 In this study, a comprehensive integrated design for biodiesel production process using  
123 supercritical methanol has been simulated. The reactor has been designed based on previous  
124 experimentally reported kinetic parameters. Energy and mass integration principles have  
125 been applied to reduce the process required external energy and fresh resources, respectively.  
126 Graphical Pinch method has been applied to design and develop a new optimum HEN  
127 responsible for reduction of heating and cooling required energies. In addition, it has been  
128 used to evaluate previously reported designs.

129

## 130 **2. MATERIALS AND METHODS**

131

132 The transesterification/esterification reactions for WCO were carried out using supercritical  
133 methanol. The details about the experimental design and procedures are presented elsewhere  
134 [26]. Aspen HYSYS simulation programme version 8.8 was used for simulating the biodiesel  
135 process (Aspen Technology Inc., USA). The procedures for process simulation based on  
136 HYSYS simulator consist of several steps including selection of chemical components for  
137 the process, appropriate thermodynamic models, required process units and operating  
138 conditions. The actual existing pressure drop in different equipment was neglected in the  
139 present study.

140

141 The assumptions associated with the present simulation are as follows:

142

- 143 1. The transesterification reaction steps were represented by only overall step where  
144 triglycerides (TG) are converted to fatty acid methyl esters (FAME).
- 145 2. Glycerol methanol side reaction was ignored.
- 146 3. Heat exchangers were selected as counter flow type and were simulated by a means  
147 of a shortcut module.

148

### 149 **2.1 Chemical components**

150

151 Most of the required information for chemical components used in the process design were  
152 included in HYSYS data bank library. Triolein ( $C_{57}H_{104}O_6$ ) and Trilinolein ( $C_{57}H_{98}O_6$ ) were  
153 used to represent the triglycerides exists in the WCO as they were reported as the major  
154 compositions (~86%) based on the chromatographic analysis reported elsewhere [26]. Oleic  
155 and linoleic acids have been used to represent the FFAs exist in the WCO. Methyl oleate

156 (C<sub>19</sub>H<sub>36</sub>O<sub>2</sub>) and methyl linoleate (C<sub>19</sub>H<sub>34</sub>O<sub>2</sub>) were considered as the desirable product of the  
157 reaction. Conferring to the WCO's total acid number (TAN) of 0.8 mg KOH/ g oil, the FFAs  
158 weight percentage were equivalent to 1.6%. Trilinolein component was not available in the  
159 HYSYS data bank library where it has been introduced as a hypo-component using hypo-  
160 manager tool by identifying its physicochemical properties [27].

161

## 162 **2.2. Thermodynamic model**

163

164 Owing to the presence of polar components in the process, i.e.; methanol and glycerol, non-  
165 random two liquid (NRTL) activity model was selected as the fluid thermodynamic package  
166 for the activity coefficient calculations [28]. Some binary interaction coefficients were not  
167 available in the HYSYS data bank library. Accordingly, the missing coefficients were  
168 estimated using UNIFAC liquid-liquid equilibrium and UNIFAC vapour-liquid equilibrium  
169 methods. Since the activity coefficient based model such as NRTL is not recommended to be  
170 used at pressure greater than 1000 kPa, Peng-Robinson equation of state (EOS) was used in  
171 the process streams at high pressure and at separating units [10].

172

## 173 **2.3. Plant capacity, unit operations and operating conditions**

174

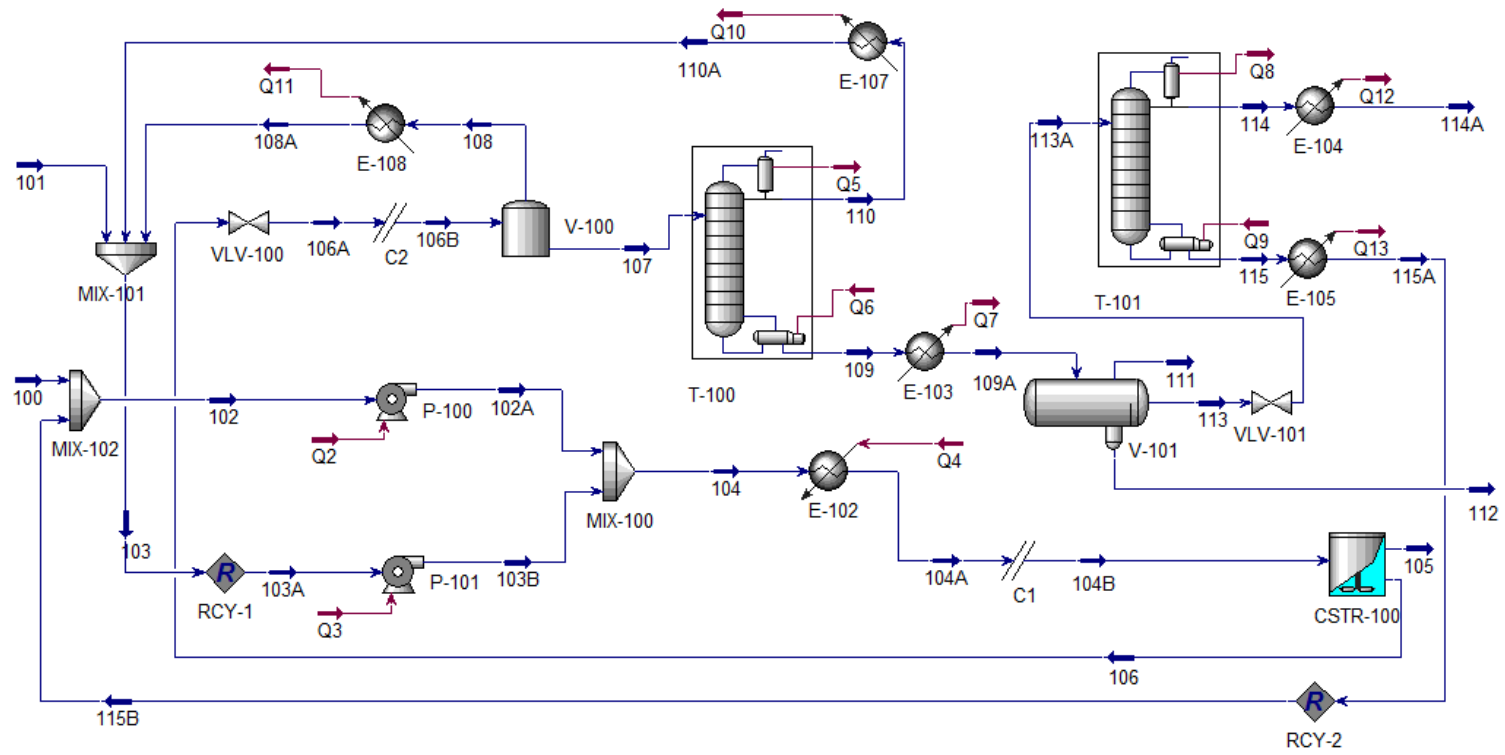
175 The biodiesel plant capacity was specified by 9.2 kgmol/h of fresh WCO feed. Conversion  
176 reactor unit exists in the simulation environment, which requires only the final reaction  
177 conversion, used in most of the process designs in the literature was replaced by kinetic  
178 continuous stirred tank reactor (CSTR) reactor. Kinetic and thermodynamic data required for  
179 the reactor including reaction rate constant (k), activation energy and frequency factor, were  
180 identified based on previous reported experimental data as of 0.0006 s<sup>-1</sup>, 50.5 kJ/mol and  
181 4.05 s<sup>-1</sup>, respectively [26]. Reactor operating conditions were identified based on the  
182 experimentally concluded optimum conditions reported previously, i.e. methanol to oil  
183 (M:O) molar ratio of 37:1, reaction temperature of 253°C, reaction pressure of 198.5 bar in  
184 14.8 minutes reaction time [26]. The process units include reactor, distillation columns, flash  
185 drum, heat exchangers and pumps.

186

187 **3. PROCESS DESIGN**

188

189 Biodiesel production process consists of several process stages including reactants  
190 preparation, transesterification/esterification reactions, methanol recovery and finally  
191 biodiesel purification. The process has been designed as a modified version for a previous  
192 process design reported by Lee et al [10]. Methanol and WCO have been pressurised and  
193 then heated to the specified conditions; then both reactants have been mixed and fed to the  
194 reactor. The reactor product stream has been depressurised and proceeded for further  
195 biodiesel purification units. Reactor product stream (Stream 106) has been processed to a  
196 simulation tool called “Cutter” which has changed the thermodynamic model from NRTL to  
197 Peng-Robinson. Fresh reactants streams for both WCO and methanol were labelled as 100  
198 and 101. Products’ streams including glycerol and biodiesel were labelled as 112 and 114A,  
199 respectively. Process flowsheet is presented in Figure 1 and the properties of main streams  
200 are given in Tables 1 and 2. A summary of the units’ operating conditions is presented in  
201 Table 3.



202  
203

Figure 1. Process flowchart for biodiesel production (numbers below streams refer to stream names)



Table 1. Stream table for the designed process (Part 1)

<b>Name</b>	<b>100</b>	<b>101</b>	<b>102</b>	<b>103</b>	<b>104A</b>	<b>105</b>	<b>106</b>	<b>107</b>
<b>Temperature (°C)</b>	25	25	25	62	253.5	230	230	87.92
<b>Pressure [kPa]</b>	101	101	101	101	19850	19840	19840	105
<b>Molar Flow [kmol/h]</b>	9.2	27	11.3	386	397.3	0	397.3	53.59
<b>Mole fractions</b>								
<b>Triolein</b>	0.6935	0	0.618	0	0.017	0	0.0016	0.0118
<b>Trilinolein</b>	0.2583	0	0.23	0	0.0066	0	0.0006	0.0044
<b>Methanol</b>	0	1	0	0.922	0.848	0	0.7809	0.2271
<b>Methyl oleate</b>	0	0	0.11	0	0.003	0	0.0522	0.3869
<b>Methyl linoleate</b>	0	0	0.001	0.002	0.0003	0	0.0185	0.1356
<b>Linoleic acid</b>	0.0131	0	0.011	0	0.0003	0	0	0.0002
<b>Oleic acid</b>	0.0351	0	0.03	0	0.0009	0	0.0001	0.0004
<b>Glycerol</b>	0	0	0	0	0	0	0.0220	0.1634
<b>Water</b>	0	0	0	0.076	0.123	0	0.1241	0.0701

Table 2. Stream table for the designed process (Part 2)

<b>Name</b>	<b>108A</b>	<b>109</b>	<b>110</b>	<b>111</b>	<b>112</b>	<b>113</b>	<b>114A</b>	<b>115A</b>
<b>Temperature (°C)</b>	65	254	72.3	25	25	25	25	25
<b>Pressure [kPa]</b>	101	112	101	101	101	101	101	101
<b>Molar Flow [kmol/h]</b>	343.7	37.97	15.62	0	8.809	29.16	27	1.17
<b>Mole fractions</b>								
<b>Triolein</b>	0	0.016	0	0	0	0.0619	0	0.72
<b>Trilinolein</b>	0	0.006	0	0	0	0.0229	0	0.22
<b>Methanol</b>	0.868	0.008	0.76	0	0.006	0.0009	0.008	0
<b>Methyl oleate</b>	0	0.546	0	0	0	0.6775	0.722	0.04
<b>Methyl linoleate</b>	0	0.192	0	0	0	0.2358	0.27	0
<b>Linoleic acid</b>	0	0.0002	0	0	0	0.0003	0	0
<b>Oleic acid</b>	0	0.0006	0	0	0	0.0007	0	0.02
<b>Glycerol</b>	0	0.2306	0	0	0.994	0	0.0001	0
<b>Water</b>	0.132	0.0001	0.24	0	0	0	0	0

Table 3. Summary of units operating conditions of each process

<b>Operating parameter</b>	<b>Value</b>
<b>Reactor (CSTR-100)</b>	
Temperature (°C)	253.5
Pressure (bar)	198.5
Methanol:Oil molar ratio	37:1
Residence time (min)	14.8
Conversion (%)	91.7
<b>Methanol Separating Column (T-100)</b>	
Reflux ratio	1
Number of stages	10
Condenser pressure (kPa)	101
Reboiler pressure (kPa)	112
Methanol recovery	97.8%
Distillate flowrate (kgmol/h)	16.57
Distillate purity (wt%)	84.5
<b>FAME Separating Column (T-101)</b>	
Reflux ratio	1
Number of stages	10
Condenser pressure (kPa)	2
Reboiler pressure (kPa)	5
Distillate flowrate (kgmol/h)	27
Distillate purity (wt %)	99.89

### 210 **3.1. Non-catalytic reactor**

211

212 The reactor feed stream (Stream 104A) has been pre-processed to the reaction conditions i.e.  
213 temperature of 253.5°C and pressure of 198.5 bar. The volume of the reactor has been  
214 identified based on the experimental optimum time of reaction and the flow rate of the  
215 reactants where the residence time of the reaction has been adjusted at 14.8 minutes.  
216 Consequently, the reactor has resulted in 91.7% conversion of both triolein and trilinolein to  
217 methyl oleate and methyl linoleate as similarly reported elsewhere [26]. Esterification  
218 reactions of FFAs i.e. oleic and linoleic acids to methyl oleate and methyl linoleate,  
219 respectively, have been included to the reaction set. Reaction product stream (Stream 106)  
220 has been processed for further separation unit to separate methyl oleate from unreacted  
221 components and side products.

222

223 In addition, a sensitivity analysis has been performed to investigate the effect of the variation  
224 of  $k$  on the simulated conversion in the kinetic reactor. It has been reported previously [26]  
225 that the reaction is pseudo first order and the value of  $k$  is  $0.0006 \text{ s}^{-1}$  at 253.5°C. Moreover,  
226 frequency factor and activation energy have been reported as  $4.05 \text{ s}^{-1}$  and 50.5 kJ/mol,  
227 respectively within the temperature range between 240°C and 280°C. Accordingly, a  
228 variation of  $\pm 0.0001$  of the value  $k$  has been applied, where new values of activation energy  
229 and frequency factor have been determined. Using the new values of  $k$ , activation energy and  
230 frequency factor have been varied within ranges of 44.26-58.97 kJ/mol and  $3.01\text{-}6.08 \text{ s}^{-1}$ ,  
231 respectively resulting in a significant variation of the simulated conversion results between  
232 ranges of 70.1-97.2 %. The results of this analysis could highlight the high sensitivity of the  
233 simulated conversion based on the kinetic data. Hence, it is highly recommended to perform  
234 accurate experimental kinetic calculations.

235

### 236 **3.2. Separation of unreacted methanol**

237

238 The actual M:O molar ratio (37:1) used in the reactor is much higher than the stoichiometric  
239 requirements for both transesterification of triglycerides (3:1) and esterification of FFAs  
240 (1:1). Accordingly, the product stream includes huge excess of unreacted methanol. Reactor  
241 product stream (Stream 106) has been de-pressurised to the atmospheric pressure using an  
242 expansion valve (VLV-100), where the enthalpy difference of the mixture has converted  
243 some of the liquid methanol to the vapour state. The de-pressurised product stream (Stream  
244 106D) has been fed to a flash drum (V-100) which has separated different liquid and gas

245 phases. The top product stream (Stream 108) composed mainly from methanol in addition to  
246 water. However, the bottom liquid stream (Stream 107) contains mixture of reactions  
247 products and unreacted reactants as shown in Table 1. The adiabatic flash drum has separated  
248 96% of the unreacted methanol from the reactor product stream (Stream 106).

249  
250 Further methanol separation has been carried out using a distillation column (T-100) with 10  
251 stages to provide sufficient separation [10]. Using distillation column, 97.8% of the unreacted  
252 methanol in the feed stream (Stream 107) has been separated in the top product stream  
253 (Stream 110). The bottom product (Stream 109), which mainly consists of unreacted  
254 triglycerides, produced methyl esters, fatty acids and glycerol, as shown in Table 1, has left  
255 the column at 253.9°C and cooled to 25°C for further separation processes. The unreacted  
256 methanol could be completely separated at temperatures higher than 278°C. However, the  
257 column's reboiler temperature has not exceeded 253.9°C for several reasons including  
258 avoiding thermal degradation of FAMES that shows only stability up to 270°C [29] and  
259 avoiding having traces of vaporised glycerol at the top stream where its boiling temperature  
260 is 280°C. In addition, increasing the temperature from 253.9°C to 270°C has no significant  
261 increase in methanol recovery.

262

### 263 **3.3. Glycerol separation**

264

265 Separation of glycerol from biodiesel is considered as an essential purification step as the  
266 high content of glycerol could lead to storage problems due to phase separation, higher  
267 emission of aldehyde in combustion process and clogging of the fuel injector [30]. The  
268 separation processes that have been reported in previous studies involved several techniques  
269 including gravity settling and washing with water [13]. In this work, gravity settling using  
270 phase separator has been applied. The cooled bottom product stream from distillation column  
271 (Stream 109A) has been fed to the settling unit (phase separator). Glycerol has been separated  
272 in the bottom product stream (Stream 112), where biodiesel associated with the unreacted  
273 triglycerides has been separated in the middle product stream (Stream 113). About 99.9% of  
274 glycerol in the feed stream (Stream 109A) has been separated in bottom stream (Stream 112)  
275 associated with traces of unreacted methanol. Finally, as the influent stream to the separator  
276 does not include any gases, nothing has been reported at the top product stream (Stream 111).

277

278

279

### 280 **3.4. Biodiesel purification**

281

282 According to the European standard for biodiesel specifications, EN14214, maximum  
283 concentration of triglycerides in the pure biodiesel is 0.2% by weight [10]. In this study, the  
284 glycerol free biodiesel mixture stream (Stream 113) contains 8.38% by weight of  
285 triglycerides, where it exceeds the specification of EN14214. Accordingly, further  
286 purification process has been applied for biodiesel mixture stream in order to separate the  
287 residuals of triolein. Vacuum distillation unit (VDU) has been used to avoid any thermal  
288 cracking or degradation of FAMES. Imahara et al [29] have reported that at high temperature,  
289 FAMES show stability up to 270°C, while beyond this temperature FAME starts to  
290 decompose due to isomerisation from *cis*-form to *trans*-form.

291 The feed stream has been de-pressurised using vacuum pump, which has been represented in  
292 the simulation environment as an expansion valve tool (VLV-101). Ten stages column has  
293 been used for the separation process [10]. The purified biodiesel stream (Stream 114) exits  
294 the column with less than 0.02% by weight of triolein, which is in agreement with the  
295 European standard biodiesel specifications, EN14214.

296

### 297 **4. PROCESS INTEGRATION**

298 Conservation of mass and energy in the developed industries has been considered as the most  
299 effective approach for sustainable design. Hence, implementation of HEN and MEN has  
300 gained a great interest in process engineering research through the last decades. The  
301 highlights of these researches are to minimise the external usage of energy, minimise waste  
302 discharge, minimise purchasing of fresh resources and to maximise the production of the  
303 desired product. All of these aspects are implemented through both energy and mass  
304 integration for the designed processes [23]

305

#### 306 **4.1. Mass integration**

307

308 In the present study, the designed process has been subjected to different mass integration  
309 aspects. Firstly, optimising the reaction conditions has been applied experimentally as  
310 reported previously [26] by maximising the desired product and minimising reaction  
311 conditions. In addition, mass integration principles have been applied for the developed  
312 process. As the designed process did not include any mass exchanging units, mass integration  
313 would be only highlighted through minimising waste and fresh resources. The fresh resources  
314 used for this process are WCO and methanol. Methanol is considered as a major reactant,  
315 which is used in large excess in the non-catalytic transesterification reaction. Hence,  
316 minimising fresh and waste methanol is considered as an essential requirement for biodiesel  
317 integrated process.

318 In the existing process, two available sources streams for methanol have been observed  
319 including streams separated from both adiabatic flash drum unit and distillation column unit,  
320 i.e.; streams 108 and 110. On the other hand, there is only one sink that require fresh  
321 methanol, which is the reactor (CSTR-100). The required flowrate of fresh methanol for the  
322 process sink is 386 kgmol/h which is a massive amount to be purchased. Moreover, the  
323 reactor requires huge excess of methanol where waste methanol is considerably high.  
324 Consequently, using simple source-sink mapping shown in Figure 2, a proposed scheme for  
325 methanol recycling has been developed. The reactor required methanol with maximum  
326 composition of impurities of 5% where the available sources are having much lower  
327 impurities (<1%). Accordingly, simple recovery for both available sources has been  
328 implemented as shown in the process flow chart shown in Figure 1, where both sources  
329 streams have been mixed directly with the minimum required fresh methanol stream to be  
330 fed to the reactor. After applying this mass integration recycling, the actual fresh methanol  
331 used is only 27 kgmol/h (Stream 101) instead of 386 kgmol/h in case of having no recycling  
332 approach which represents 93% savings for the fresh methanol requirements.

333

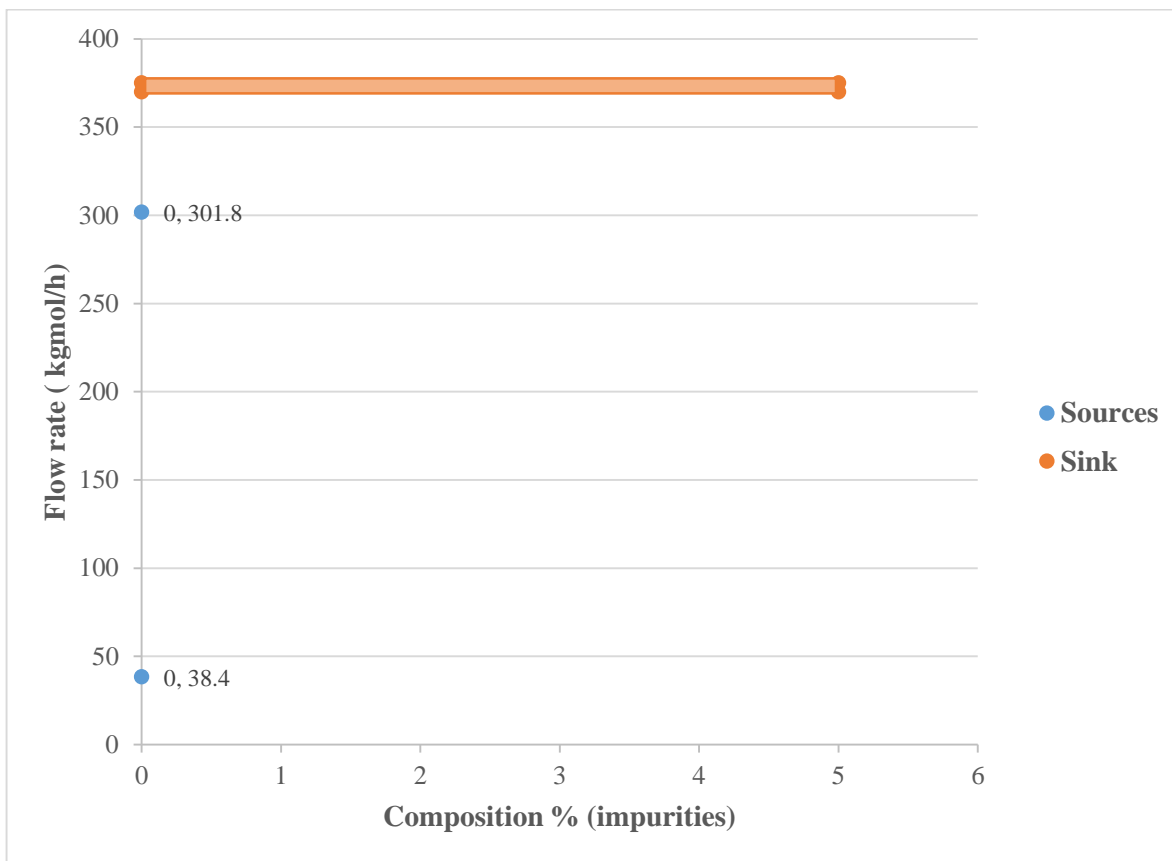


Figure 2. Source-sink mapping

334  
 335  
 336  
 337  
 338  
 339  
 340  
 341  
 342  
 343  
 344  
 345  
 346  
 347

#### 4.2. Heat integration

Pinch technology has been used to integrate the energy required for both heating and cooling for all process streams. The list of the process hot and cold streams has been presented in Table 4. An assumption of  $\Delta T_{\min}$  of 10°C has been proposed. Identifying Pinch temperatures would be proceeded using either problem table algorithm and/or heat composite curve. In the present study, the Pinch temperatures have been identified using the second method. Aspen Energy Analyzer<sup>®</sup> V8.8 simulation software has been used in identify the Pinch temperatures, minimum heating and cooling energy requirements and plotting composite curve for the process streams.



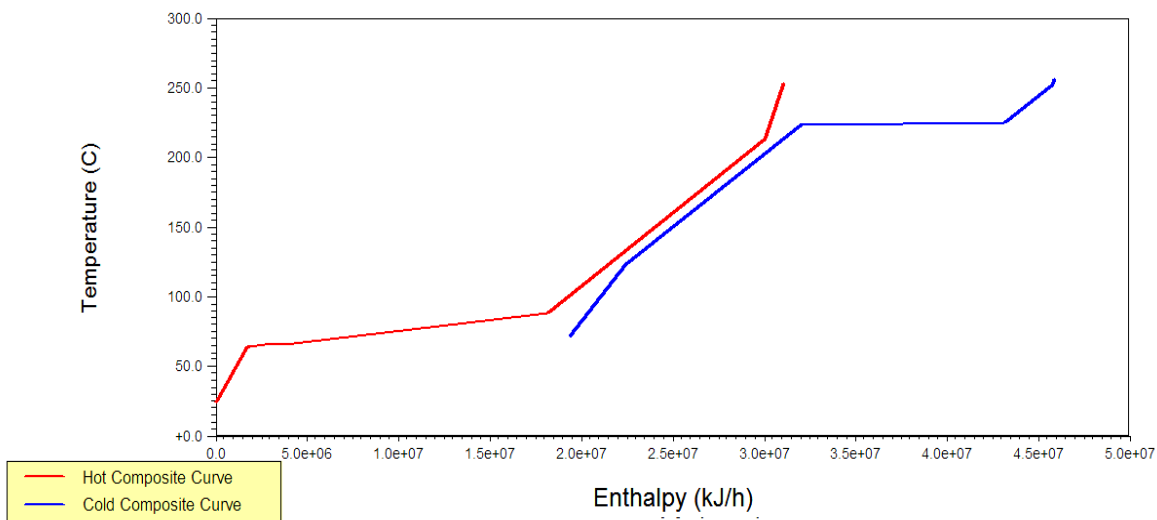
348

Table 4. Process hot and cold streams

Stream	Hot/Cold	Inlet T (°C)	Outlet T (°C)	C <sub>p</sub> (kJ/kg.°C)	Heat duty (×10 <sup>6</sup> kJ/h)
104	←	72.6	253.5	6.076	10.550
REB1	←	124.1	256.4	3.053	4.9560
REB2	←	224.5	226	176.660	10.960
108	→	89	65	1,633.100	12.800
109	→	253.9	25	2.416	5.858
110	→	66.5	65	3.687	0.002
114	→	80.4	25	2.009	0.622
115	→	241.3	25	1.510	0.441
COND1	→	66.5	66.4	9,012.800	0.961
COND2	→	214.1	63.7	4.195	10.100

349

350 A composite curve for the process streams has been developed as shown in Figure 3. The  
 351 overlap between hot and cold composite curves represents the prospective integration  
 352 between hot and cold streams according to Pinch rules [31]. The minimum energies required  
 353 for both heating (Q<sub>h</sub>) and cooling (Q<sub>c</sub>) have been observed from Figure 3 as 4,108 kW and  
 354 5,400 kW, respectively.

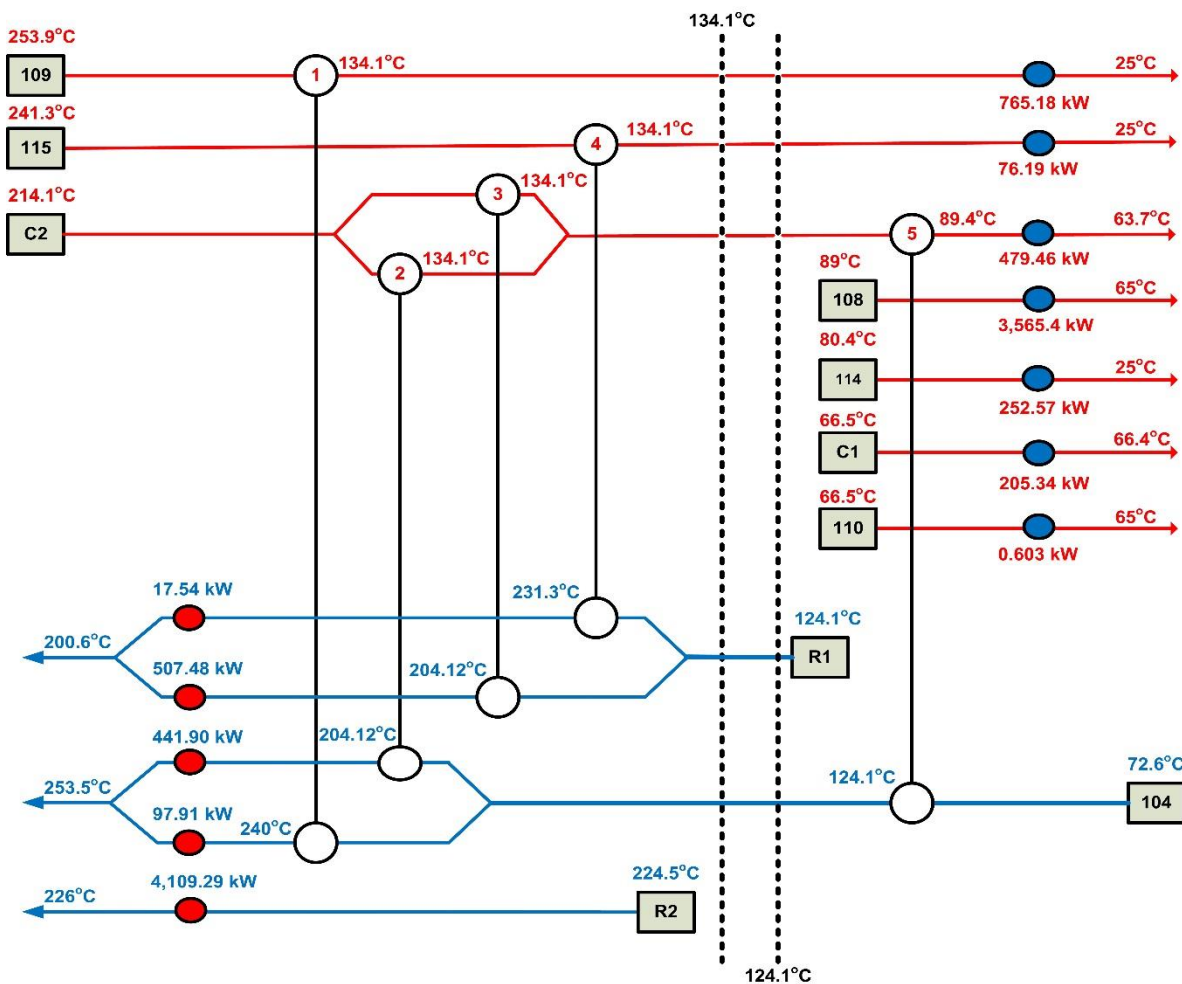


355

356

Figure 3. Composite curve of the process streams

357 In an attempt to minimise the process energy consumption and increase energy integration  
 358 between process streams, design of a new HEN design has been developed using graphical  
 359 Pinch Analysis method using only 5 heat exchangers as shown in Figure 4. Using numerical  
 360 matching in graphical method eases the process of exchanger streams' selection and streams  
 361 splitting. In addition, it investigates the validity of the exchangers according to Pinch rules.  
 362 The designed exchangers have been analysed graphically where the exchangers fulfil the  
 363 method guidelines as shown in Figure 5. The graphical method shortened the trial procedures  
 364 that would be applied to achieve the optimum network using conventional Pinch methods.  
 365 Consequently, the developed HEN has resulted in achieving 100% of both minimum heating  
 366 and cooling energies requirements.



368  
 369

Figure 4. Heat exchanger network designed for the integrated process

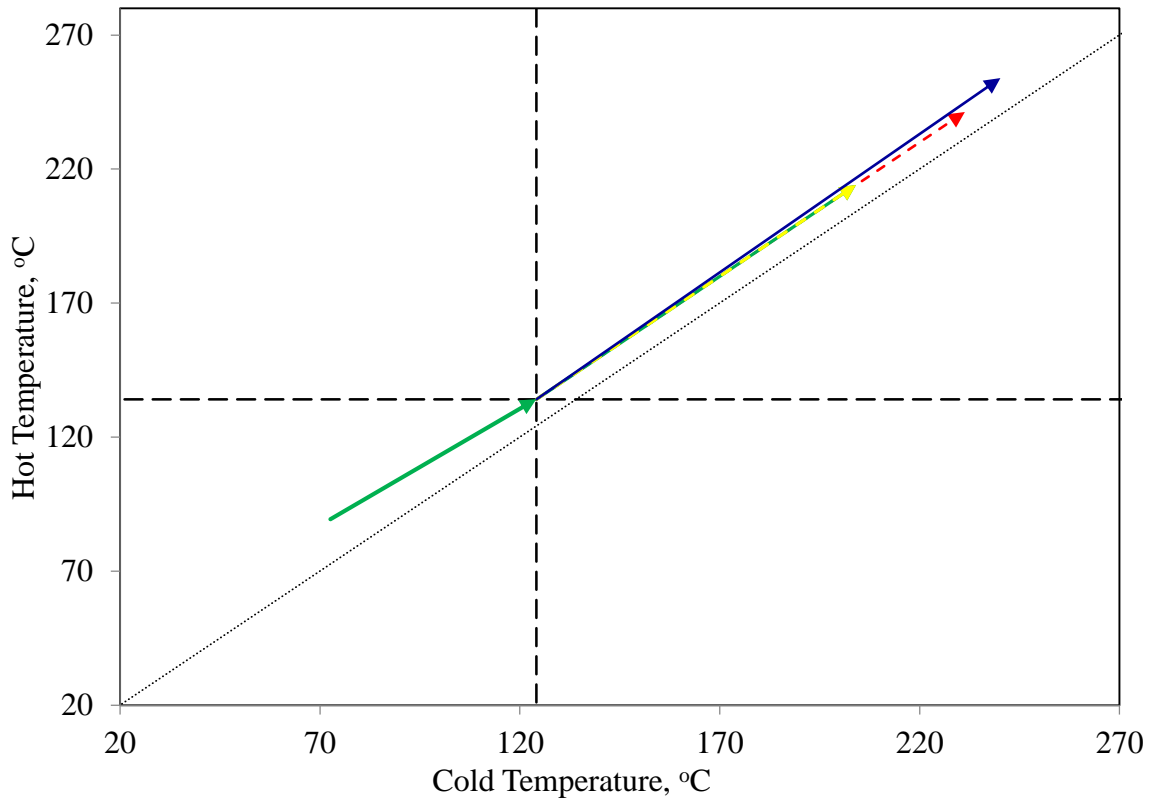
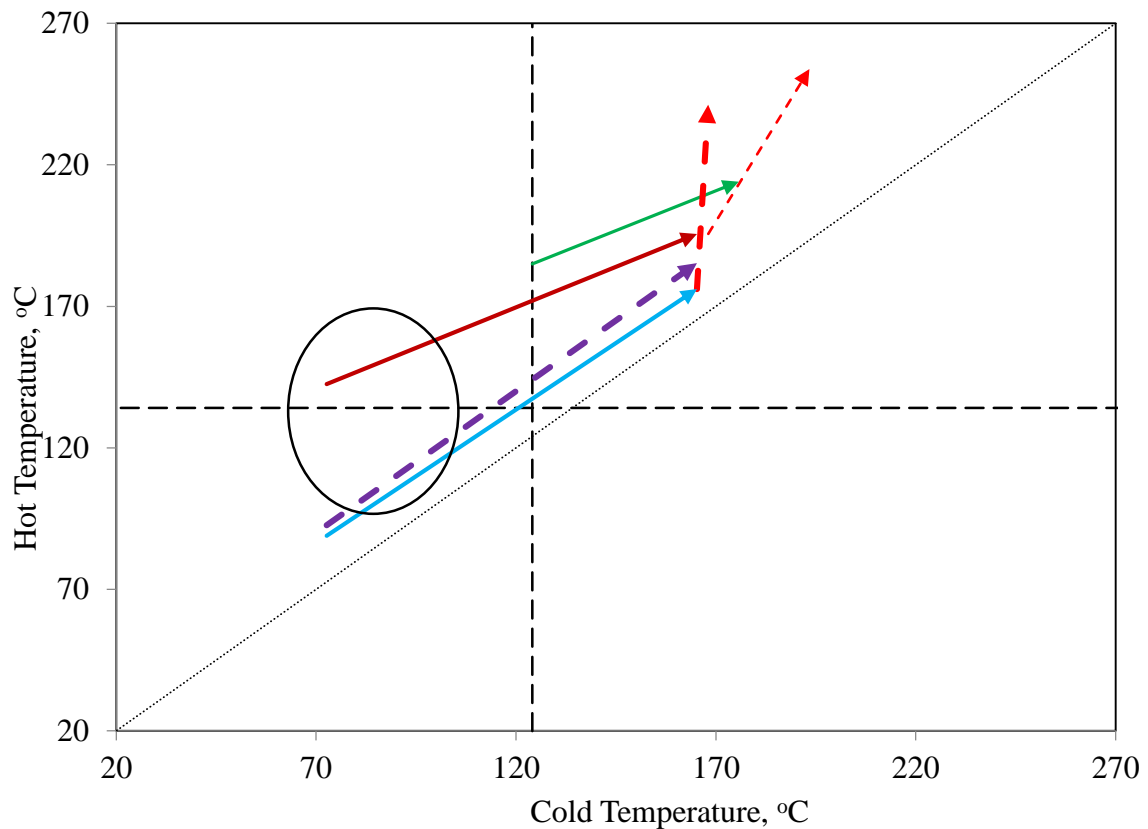


Figure 5. Graphical representation of the designed HEN on T-T diagram

370  
 371  
 372  
 373  
 374  
 375  
 376  
 377  
 378  
 379  
 380  
 381  
 382

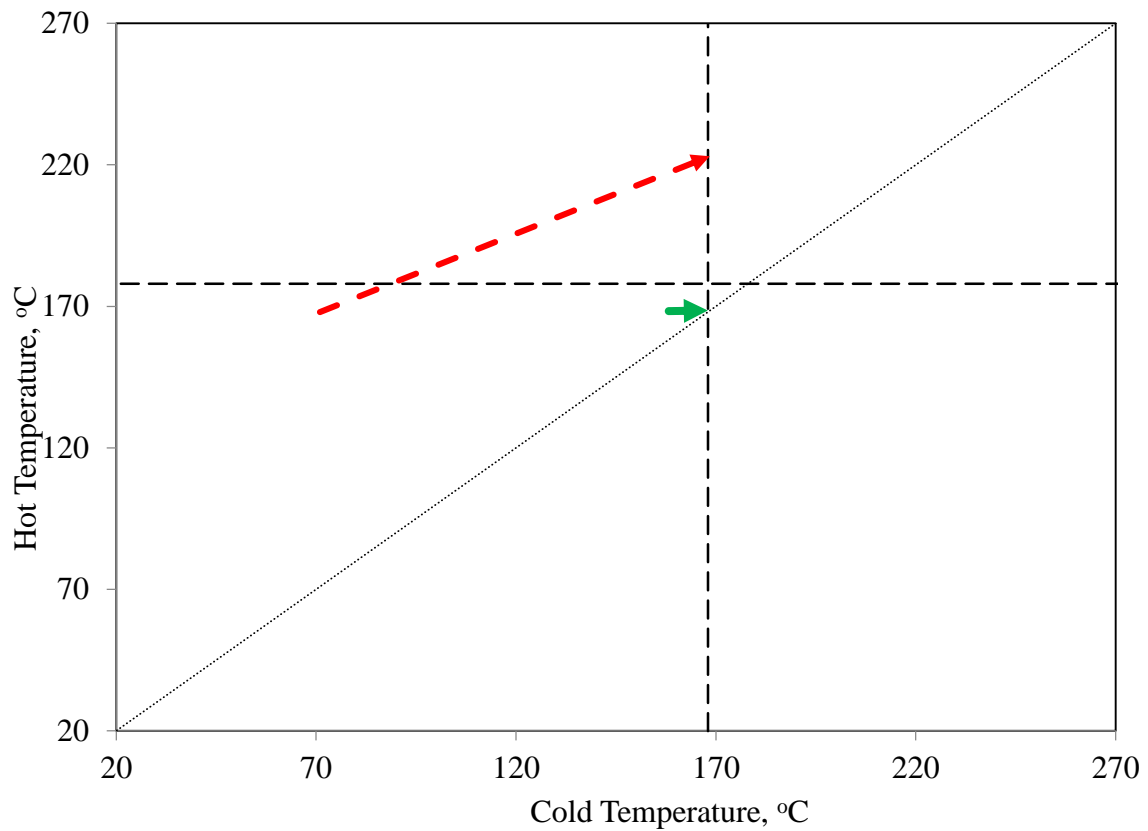
These results have been compared with the automated designs developed by Aspen Energy Analyzer software. It has been observed that the optimum automated design has used 6 heat exchangers and achieved 118% and 113.9% of the minimum heating and cooling energies requirements, respectively. This implies that the automated design consumes more energy than the targets. Graphical Pinch method has been used to investigate the proposed automated design and to highlight the problems associated with the design using simple and quick observations. Figure 6 illustrates a graphical representation of the proposed design using graphical Pinch method on T-T plot. It could be easily observed that 3 of the proposed automated exchangers are existing within the non-optimum integration area where a revamping design is required to relocate the exchangers within the optimum integrating areas.



383  
 384  
 385  
 386  
 387  
 388  
 389  
 390  
 391  
 392  
 393  
 394  
 395  
 396  
 397

Figure 6. Graphical representation of the automated proposed HEN on T-T diagram

Lee et al [10] have designed an energy integrated process for biodiesel using supercritical methanol. They have included only 2 heat exchangers to the process HEN. Their developed HEN has been also analysed using graphical Pinch method as shown in Figure 7. The simple designed HEN includes two exchangers with major problems. The first exchanger is a network Pinch exchanger where the developed straight line representing the exchanger touches the Pinch line as shown in Figure 7. This elaborates that the exchanger is not fulfilling Pinch rules with insufficient minimum heat transfer temperature difference. When an exchanger touches the Pinch line, it indicates that the process streams temperature difference is equal to zero and accordingly, an inefficient exchanger. On the other hand, the second exchanger has been included within the non-optimum integration area and the temperatures are crossing the Pinch line.



398  
 399  
 400  
 401  
 402  
 403  
 404  
 405  
 406  
 407

Figure 7. Graphical representation of the literature proposed HEN on T-T diagram

These results exemplify the significance of using graphical Pinch method in analysing existing HENs where the inefficient exchangers would be easily observed. In addition, using graphical matching technique for process streams simplify the integration procedures where it could be implemented to match many streams in relatively short time compared with the conventional methods.

## 408 5. CONCLUSIONS

409 In this work, an integrated process for non-catalytic biodiesel production from WCO using  
410 supercritical methanol has been simulated. The process has been designed where the  
411 produced biodiesel relies in agreement with the European Standard for biodiesel  
412 specifications, EN14214. The developed process has been subjected to both mass and energy  
413 integration to minimise the fresh methanol requirements and to minimise the external  
414 required energies for heating and cooling, respectively. Methanol recycling strategies have  
415 contributed to minimise fresh required methanol. Graphical Pinch method has been  
416 implemented to design an optimum HEN using numerical matching strategy. The designed  
417 HEN has achieved 100% of the targeted optimum required energies.

418

## 419 ACKNOWLEDGMENT

420

421 The authors would like to acknowledge The British Council UK and STDF Egypt through  
422 the Institutional Links Newton-Mosharafa Programme (Project IDs 261862377 and 27738)  
423 for funding this research.

424

## 425 REFERENCES

426

- 427 [1] Đurišić-Mladenović N, Kiss F, Škrbić B, Tomić M, Mičić R, Predojević Z. Current  
428 state of the biodiesel production and the indigenous feedstock potential in Serbia.  
429 *Renew Sustain Energy Rev* 2018;81:280–91. doi:10.1016/j.rser.2017.07.059.
- 430 [2] Kumar M, Sharma MP. Selection of potential oils for biodiesel production. *Renew*  
431 *Sustain Energy Rev* 2016;56:1129–38. doi:10.1016/j.rser.2015.12.032.
- 432 [3] Abidin SZ, Haigh KF, Saha B. Esterification of free fatty acids in used cooking oil  
433 using ion-exchange resins as catalysts: An efficient pretreatment method for biodiesel  
434 feedstock. *Ind Eng Chem Res* 2012;51:14653–64. doi:10.1021/ie3007566.
- 435 [4] Aboelazayem O, El-Gendy NS, Abdel-Rehim AA, Ashour F, Sadek MA. Biodiesel  
436 production from castor oil in Egypt: process optimisation, kinetic study, diesel engine  
437 performance and exhaust emissions analysis. *Energy* 2018;157:843–52.  
438 doi:https://doi.org/10.1016/j.energy.2018.05.202.
- 439 [5] Semwal S, Arora AK, Badoni RP, Tuli DK. Biodiesel production using heterogeneous  
440 catalysts. *Bioresour Technol* 2011;102:2151–61. doi:10.1016/j.biortech.2010.10.080.
- 441 [6] Farobie O, Matsumura Y. State of the art of biodiesel production under supercritical  
442 conditions. *Prog Energy Combust Sci* 2017;63:173–203.  
443 doi:10.1016/j.peccs.2017.08.001.
- 444 [7] Kiss FE, Martinovic FL, Simikic MĐ, Molnar TT. Comparative analysis of single-

- 445 step and two-step biodiesel production using supercritical methanol on laboratory-  
446 scale 2016;124:377–88. doi:10.1016/j.enconman.2016.07.043.
- 447 [8] Zhang Y, Dubé M., McLean D., Kates M. Biodiesel production from waste cooking  
448 oil: 1. Process design and technological assessment. *Bioresour Technol* 2003;89:1–16.  
449 doi:10.1016/S0960-8524(03)00040-3.
- 450 [9] Mardhiah HH, Ong HC, Masjuki HH, Lim S, Lee HV. A review on latest  
451 developments and future prospects of heterogeneous catalyst in biodiesel production  
452 from non-edible oils. *Renew Sustain Energy Rev* 2017;67:1225–36.  
453 doi:10.1016/j.rser.2016.09.036.
- 454 [10] Lee S, Posarac D, Ellis N. Process simulation and economic analysis of biodiesel  
455 production processes using fresh and waste vegetable oil and supercritical methanol.  
456 *Chem Eng Res Des* 2011;89:2626–42. doi:10.1016/j.cherd.2011.05.011.
- 457 [11] Aboelazayem O, Abdelaziz O, Gadalla M, Hulteberg C, Saha B. Biodiesel production  
458 from high acid value waste cooking oil using supercritical methanol: Esterification  
459 kinetics of free fatty acids. *Eur. Biomass Conf. Exhib. Proceedings, EUBCE2017, (12-  
460 15 June), 2017, p. 1381–7.*
- 461 [12] Farobie O, Leow ZYM, Samanmulya T, Matsumura Y. In-depth study of continuous  
462 production of biodiesel using supercritical 1-butanol. *Energy Convers Manag*  
463 2017;132:410–7. doi:10.1016/j.enconman.2016.09.042.
- 464 [13] West AH, Posarac D, Ellis N. Assessment of four biodiesel production processes using  
465 HYSYS.Plant. *Bioresour Technol* 2008;99:6587–601.  
466 doi:10.1016/j.biortech.2007.11.046.
- 467 [14] Manuale DL, Torres GC, Vera CR, Yori JC. Study of an energy-integrated biodiesel  
468 production process using supercritical methanol and a low-cost feedstock. *Fuel  
469 Process Technol* 2015;140:252–61. doi:10.1016/j.fuproc.2015.08.026.
- 470 [15] Umeda T, Itoh J, Shiroko K. Heat Exchange Systems Synthesis. *Chem Eng Prog*  
471 1978;74:70–6.
- 472 [16] Linnhoff B, Hindmarsh E. The Pinch Design Method for Heat Exchanger Networks.  
473 *Chem Eng Sci* 1983;38:745–63. doi:10.1016/0009-2509(83)80185-7.
- 474 [17] Smith R. *Chemical Process Design and Integration*. 2005, John Wiley and Sons Ltd.,  
475 Sussex, England. doi:10.1529/biophysj.107.124164.
- 476 [18] Gadalla MA. A novel graphical technique for Pinch Analysis applications: Energy  
477 Targets and grassroots design. *Energy Convers Manag* 2015;96:499–510.  
478 doi:10.1016/j.enconman.2015.02.079.
- 479 [19] El-Halwagi MM. Synthesis of Combined Heat and Reactive Mass-Exchange  
480 Networks. *Sustain Des Through Process Integr* 2017:431–9. doi:10.1016/B978-0-12-  
481 809823-3.00017-5.
- 482 [20] Klemeš JJ, Kravanja Z. Forty years of Heat Integration: Pinch Analysis (PA) and  
483 Mathematical Programming (MP). *Curr Opin Chem Eng* 2013;2:461–74.  
484 doi:10.1016/j.coche.2013.10.003.

- 485 [21] Ahmetović E, Ibrić N, Kravanja Z, Grossmann IE, Maréchal F, Čuček L, et al.  
486 Simultaneous optimisation and heat integration of evaporation systems including  
487 Mechanical Vapour Recompression and background process. *Energy* 2018.  
488 doi:10.1016/j.energy.2018.06.046.
- 489 [22] El-Halwagi MM. Mathematical Techniques for the Synthesis of Heat-Exchange  
490 Networks. *Sustain Des Through Process Integr* 2017;417–29. doi:10.1016/B978-0-12-  
491 809823-3.00016-3.
- 492 [23] Klemeš JJ. Handbook of Process Integration (PI): Minimisation of Energy and Water  
493 Use, waste and emissions, 2013, Woodhead Publishing Ltd, Cambridge, UK.  
494 doi:10.1533/9780857097255.
- 495 [24] Gadalla MA. A new graphical method for Pinch Analysis applications: Heat  
496 exchanger network retrofit and energy integration. *Energy* 2015;81:159–74.  
497 doi:10.1016/j.energy.2014.12.011.
- 498 [25] Gadalla MA. A new graphical-based approach for mass integration and exchange  
499 network design. *Chem Eng Sci* 2015;127:239–52. doi:10.1016/j.ces.2015.01.036.
- 500 [26] Aboelazayem O, Gadalla M, Saha B. Biodiesel production from waste cooking oil via  
501 supercritical methanol: Optimisation and reactor simulation. *Renew Energy*  
502 2018;124:144–54. doi:10.1016/j.renene.2017.06.076.
- 503 [27] Plazas-González M, Guerrero-Fajardo CA, Sodr e JR. Modelling and simulation of  
504 hydrotreating of palm oil components to obtain green diesel. *J Clean Prod*  
505 2018;184:301–8. doi:10.1016/j.jclepro.2018.02.275.
- 506 [28] Aboelazayem O, Gadalla M, Saha B. An Experimental-Based Energy Integrated  
507 Process for Biodiesel Production from Waste Cooking Oil Using Supercritical  
508 Methanol. *Chem Eng Trans* 2017;61:1645–50. doi:10.3303/CET1761272.
- 509 [29] Imahara H, Minami E, Hari S, Saka S. Thermal stability of biodiesel in supercritical  
510 methanol. *Fuel* 2008;87:1–6. doi:10.1016/j.fuel.2007.04.003.
- 511 [30] Santana GCS, Martins PF, de Lima da Silva N, Batistella CB, Maciel Filho R, Wolf  
512 Maciel MR. Simulation and cost estimate for biodiesel production using castor oil.  
513 *Chem Eng Res Des* 2010;88:626–32. doi:10.1016/j.cherd.2009.09.015.
- 514 [31] Farrag N, Gadalla M, Fouad M. Reaction parameters and an energy optimization for  
515 biodiesel production using a supercritical process. *Chem Eng Trans* 2016;52:1207–12.  
516 doi:10.3303/CET1652202.
- 517